Journal of Autoimmunity 101 (2019) 1–16

Contents lists available at ScienceDirect

Journal of Autoimmunity

journal homepage: www.elsevier.com/locate/jautimm

A cell type-specific transcriptomic approach to map B cell and monocyte type I interferon-linked pathogenic signatures in Multiple Sclerosis

Martina Severa[a,*], Fabiana Rizzo[a], Sundararajan Srinivasan[b], Marco Di Dario[b], Elena Giacomini[a], Maria Chiara Buscarinu[c], Melania Cruciani[a], Marilena P. Etna[a], Silvia Sandini[a], Rosella Mechelli[c,d], Antonella Farina[e], Pankaj Trivedi[e], Paul J. Hertzog[f], Marco Salvetti[c,g], Cinthia Farina[b], Eliana M. Coccia[a,**]

[a] Department of Infectious Diseases, Istituto Superiore di Sanità, Rome, Italy
[b] Institute of Experimental Neurology (INSpe), Division of Neuroscience, San Raffaele Scientific Institute, Milan, Italy
[c] Center for Experimental Neurological Therapies, Sant'Andrea Hospital, Department of Neurosciences, Mental Health and Sensory Organs, Sapienza University, Rome, Italy
[d] Department of Human Science and Promotion of Quality of Life, San Raffaele Roma Open University and IRCCS San Raffaele-Pisana, Rome, Italy
[e] Department of Experimental Medicine, Sapienza University, Rome, Italy
[f] Department of Molecular and Translational Sciences, Monash University, Clayton, Australia
[g] Istituto Neurologico Mediterraneo (INM) Neuromed, Pozzilli, Isernia, Italy

ARTICLE INFO

Keywords:
Relapsing-remitting multiple sclerosis
B cell
Monocyte
Transcriptome
Interferome
Apoptosis
Antiviral state
Type I interferon signaling

ABSTRACT

Alteration in endogenous Interferon (IFN) system may profoundly impact immune cell function in autoimmune diseases.

Here, we provide evidence that dysregulation in IFN-regulated genes and pathways are involved in B cell- and monocyte-driven pathogenic contribution to Multiple Sclerosis (MS) development and maintenance.

In particular, by using an *Interferome*-based cell type-specific approach, we characterized an increased susceptibility to an IFN-linked caspase-3 dependent apoptotic cell death in both B cells and monocytes of MS patients that may arise from their chronic activation and persistent stimulation by activated T cells. Ongoing caspase-3 activation functionally impacts on MS monocyte properties influencing the STAT-3/IL-16 axis, thus, driving increased expression and massive release of the bio-active IL-16 triggering and perpetuating $CD4^+$ T cell migration.

Importantly, our analysis also identified a previously unknown multi-component defect in type I IFN-mediated signaling and response to virus pathways specific of MS B cells, impacting on induction of anti-viral responses and Epstein-barr virus infection control in patients.

Taking advantage of cell type-specific transcriptomics and in-depth functional validation, this study revealed pathogenic contribution of endogenous IFN signaling and IFN-regulated cell processes to MS pathogenesis with implications on fate and functions of B cells and monocytes that may hold therapeutic potential.

Abbreviations: Ab, antibody; AIM2, absent in melanoma 2 gene; CNS, central nervous system; EBER-1, Epstein-barr virus-encoded small RNA; EBV, Epstein-barr virus; FBS, fetal bovine serum; FvDye, Fixable viability dye; GO, gene ontology; HD, healthy donor; IFNAR, Interferon-α/β receptor; IFI, Interferon inducible protein; IFN, interferon; IFNGR, Interferon-γ receptor; IL-16, Interleukin-16; IL-1RA, interleukin-1 receptor antagonist; IRAK3, IL-1 receptor-associated kinase 3; IRF, Interferon regulatory factor; IRG, Interferon-regulated gene; mAb, monoclonal antibody; MS, multiple sclerosis; Mx1, Mx dynamin-like GTPase 1; MyD88, myeloid differentiation primary response gene 88; OAS1, 2′-5′ oligoadenylate synthetase 1; PBMC, peripheral blood mononuclear cells; RRMS, relapsing-remitting multiple sclerosis; SD, standard deviation; SP110, sp110 nuclear body protein gene; STAT, signal transducer and activator of transcription; TBK1, TANK binding kinase 1; TBP, TATA-box-binding protein; TLR, Toll-like receptor

** Corresponding author.
* Corresponding author.
E-mail addresses: martina.severa@iss.it (M. Severa), eliana.coccia@iss.it (E.M. Coccia).

https://doi.org/10.1016/j.jaut.2019.04.006
Received 19 February 2019; Received in revised form 8 April 2019; Accepted 8 April 2019
Available online 30 April 2019
0896-8411/

1. Introduction

Multiple sclerosis (MS) is a chronic inflammatory disorder of the central nervous system (CNS) characterized by structural and functional alterations in this tissue compartment that give rise to progressive neurodegeneration associated to disability [1,2]. Although the nature of the disease remains elusive, it was reported that MS implies a complex interaction among environmental factors (i.e. lifestyle-related and infectious agents) in a genetically susceptible host [3].

Indeed, to preserve the integrity of the host, the immune system works to distinguish self from harmful non-self. Deficits in this discrimination can result in hyper-susceptibility to infections or over-reactivity to harmless antigens, leading to immunopathology and autoimmunity. Thus, in individuals with autoimmune diseases, some pathogens may establish a more severe primary infection [4]. Many infectious agents have been proposed to have a role in MS, but one of the most interesting candidates is Epstein-barr virus (EBV), with extensive literature supporting the hypothesis that EBV infection increases the risk of MS [5,6].

Interferons (IFNs) are a pleiotropic family of cytokines protecting host organism from infection, disease and maintaining immune homeostasis [7]. Type I IFNs (mainly IFN-αs and IFN-β), in particular, are involved in the multi-level regulation of antiviral responses, while type II IFN, i.e. IFN-γ, whose expression is dramatically altered in MS, is linked to activation and perpetuation of inflammation [8,9]. Like other multifunctional cytokines, excessive or inappropriate activity of IFNs can cause toxicity and even death. Therefore, host organisms have evolved highly regulated mechanisms to select appropriate genes and pathways as effectors of the IFN response in cells and control the temporal and tissue specificity of IFN production. Recent data have uncovered a dark side to IFN in inflammatory diseases, autoimmunity and diabetes, where these mechanisms of control are significantly altered [8,9].

In MS, genome-wide association studies identified single nucleotide polymorphisms and variants involved in type I IFN signaling and antiviral pathways (such as IFN regulatory factor 8, IRF8; suppressor of cytokine signaling 1; tyrosine kinase 2; signal transducer and activator of transcription 3, STAT3; zinc finger CCCH-type containing, antiviral 1 protein and 2′-5′ oligoadenylate synthetase 1, OAS1) [10–12], which may display transcriptional dysregulation in blood cells at distinct MS stages [13]. Information on IFN signature are available for MS subjects under IFN-β therapy [14], however, these studies do not provide any insights on the state of the endogenous IFN signaling. Some studies on the antiviral state and IFN-regulated responses in therapy-free MS patients highlighted significant changes associated to MS stages and disease activity; however, these data refer to the mixed cell population of peripheral blood mononuclear cells (PBMC) [15–22].

Recent advances in the field set B cells and monocytes on the central stage in MS, as these cell types contribute to CNS-compartmentalized inflammatory responses and provide systemic disease maintenance [23–32]. In this study, by employing the *Interferome* database, containing a full collection of types I, II and III IFN-regulated genes (IRG) catalogued from published and available gene expression datasets [33,34], we have carried out an *Interferome*-filtered transcriptomic-based approach to systematically analyze alterations in endogenous IFN signaling occurring in B cells and monocytes of MS patients. The *Interferome*-based analysis followed by cell type-specific in-depth functional validation studies helped in the characterization of previously unknown dysregulation in IFN-linked pathways and cell mechanisms altered specifically in MS B cells and monocytes relevant to MS pathogenesis and maintenance.

2. Materials and methods

2.1. Enrollment of MS patients and healthy controls

For this study untreated patients with definite relapsing-remitting MS (RRMS) according to revised McDonald's criteria [35] were enrolled at S. Andrea Hospital MS Center (Sapienza University, Rome, Italy). Twenty-five were enrolled for the exploratory cohort [17 females/8 males; median age ± Standard Deviation (SD) 39 ± 1 yrs; Females: 42 ± 13 yrs, Males: 39 ± 11 yrs] (Supplementary Table 1) and thirty-five for the validation cohort (21 females/14 males; median age ± SD, 44 ± 12 yrs; Females: 46 ± 11.5 yrs, Males: 39 ± 13 yrs) (Supplementary Table 2).

Median Expanded Disability Status Scale was 1 ± 1.2 (range 0–4) for Exploratory cohort and 1 ± 1 (range 0–4) for Validation cohort. Median disease duration was 7 ± 6 (range 0.5–22 yrs) for Exploratory cohort and 6 ± 7 (range 0.5–26 yrs) for Validation cohort. Patients had not been taking steroids or any disease-modifying drugs for at least three months prior to their enrollment in the study. Additional exclusion criteria included presence of other autoimmune disorders, cancer, active infection that may be associated with abnormal immune response, and pregnancy.

Twenty-four sex- and age-matched healthy donors (HD) were also enrolled for the exploratory cohort (15 females/9 males; median age ± SD, 36 ± 7.5 yrs; Females: 36 ± 7.5 yrs, Males: 36 ± 8.5 yrs) (Supplementary Table 3) and twenty-nine for the Validation cohort (18 females/11 males; median age ± SD, 42 ± 9.4 yrs; Females: 39 ± 10 yrs, Males: 44 ± 7 yrs) (Supplementary Table 4). Inclusion criteria for this group were the absence of autoimmune diseases, cancer, active infection, pregnancy and immunomodulatory treatments.

The Ethics Committee of S. Andrea Hospital approved this study (CE 204/10). All the subjects involved in the study gave written informed consent.

2.2. Cell isolation and treatments

PBMC were isolated from peripheral blood (~40 ml), withdrawn from patients and paired HD, by density gradient centrifugation using Lympholyte-H (Cedarlane Laboratories) and cultured (1×10^6 cells/ml) in RPMI 1640 (BioWhittaker Europe) supplemented with 2 mM L-glutamine, 100 U/ml penicillin, 100 μg/ml streptomycin (Gibco) and 10% fetal bovine serum (FBS, Lonza-Biowhittaker) [36].

To isolate paired B cells and monocytes from the same patients an *ad-hoc* purification protocol was set-up by using sequentially $CD19^+$ and then $CD14^+$ magnetic microbeads (Miltenyi Biotech). Briefly, PBMC were first incubated with $CD19^+$ beads. Upon B cell purification, PBMC depleted of $CD19^+$ cells were incubated with $CD14^+$ beads to isolate monocytes. Manufacturer's protocol was implemented by modifying column washing steps and procedure of incubation to reach almost 100% purity of cells, checked for each cell preparation by flow cytometry.

Most of the experiments were conducted on freshly isolated cells (*ex vivo*). However, in the validation studies, cells were cultured at 10^6 cells/ml in RPMI 1640 (Lonza-Biowhittaker), in the presence of 1 mM penicillin and streptomycin (Lonza-Biowhittaker) and complemented with 2 mM L-glutamine (Lonza-BioWhittaker) and 10% FBS (Lonza-Biowhittaker). Staurosporine (Sigma Aldrich) was used at 1 μM in presence of the protein transport inhibitor GolgiPlug™ (BD Biosciences). *Z*-VAD-FMK caspase-3 inhibitor (Sigma Aldrich) was used at 100 μM. Intron® A (IFN-α 2 recombinant, Merck-Serono) and Rebif 44® (IFN-β1a recombinant, Merck-Serono) were used at 1 or 10 units/ml. Human recombinant IFN-γ (Peprotech) was used at 1, 10 or 100 units/ml.

2.3. FACS analysis

Flow cytometry analysis was conducted as previously described [36,37]. Briefly, 5×10^6 PBMC were stained with monoclonal antibodies (mAb) against the cell-lineage specific surface marker CD14 for monocytes (PE; BD Pharmingen, clone M5E2) and CD19 for B cells (PE-Cy™7; BD Pharmingen, clone SJ25C1). For B cells the anti-CD27 mAb (FITC; BD Pharmingen, clone M-T271) was also used to allow the discrimination of $CD19^+CD27^-$ naïve and $CD19^+CD27^+$ memory B cell subtypes.

To identify those cells undergoing apoptosis, PBMC were stained with the Annexin-V apoptosis detection reagent (Abcam).

To evaluate plasmablast differentiation and B cell proliferation in EBV-GFP cultures we stained cells with mAbs for CD19 (PE-Cy™7; BD Pharmingen, clone SJ25C1), CD27 (BrillantViolet510; Biolegend, clone O323), CD38 (APC, BD Pharmingen, clone HIT2), CD138 (VioBlue; Miltenyi Biotech) and intracellular marker Ki67 (AlexaFluor700, Biolegend, clone 16A8).

Expression of active caspase-3 was evaluated by intracellular staining with an anti-active caspase-3 mAb (Horizon V450; BD Pharmingen; clone C92-605) by using the BD Cytofix/Cytoperm Fixation/Permeabilization Kit (BD Pharmingen) according to the provided protocol.

To analyze IFN-α/β receptor chain (IFNAR) 1 and IFNAR2 surface expression in $CD19^+CD27^-$ naïve and $CD19^+CD27^+$ memory B cell subtypes, anti-human IFNAR1 mAb (APC; R&D Systems, clone 85228) and anti-human IFNAR2 mAb (PE; PBL assay science, clone MMHAR-2) were used.

MAbs' mixes always included Fixable Viability Dye (FvDye, eFluor780, eBioscience) to exclude dead cells from the analysis and the anti-CD45 mAb (Pacific Orange; Invitrogen, clone HI30) to gate lympho-mono cells only and exclude residual red blood cells. All flow cytometry analyses were conducted in $CD45^+FvDye^-$ live cells (Supplementary Fig. 1 for gating strategy).

The different IgG1 and/or IgG2a isotype negative control Abs were added as needed.

After staining, cells were fixed, where requested, with 2% paraformaldehyde and run on a FACSCanto (BD Bioscience) or on a Gallios Instrument (Beckman Coulter). Phenotypic analysis was performed using Flow Jo software (Tree Star Inc.).

2.4. RNA isolation, quantification ad quality assessment

DNase-I-treated total RNA was purified from RRMS- or HD-derived B cells and monocytes using the RNeasy Mini Kit (Qiagen, Valencia, CA) as previously described [37].

RNA was quantified using a Nanodrop spectrophotometer (Nanodrop2000) and quality assessed with an established cut-off of ~1.8 for 260/280 absorbance ratio. RNA integrity was instead inspected by Bioanalyzer analysis (Agilent Technologies) considering a cut-off of 1.8 for 28S/18S ratio.

2.5. Generation and analysis of microarray datasets

For the generation of B cell and monocyte transcriptomes cRNA were synthesized with the Illumina TotalPrep RNA Amplification kit and hybridized on Illumina Human_V4 arrays on a Beadstation 500 (Illumina). The Genome Studio GX software (Illumina) was used to extract the Illumina raw data, which were then background subtracted by NEC method and normalized by cubic spline normalization as implemented in the software. Batch effects were corrected using Combat. Probes with a mean intensity value lower than 100 in all experimental groups were filtered out. The differentially expressed genes between RRMS and HD were identified using Limma package in R.

2.6. Collection of IRG and frequency of dysregulated cell type-specific interferome in MS

The Illumina Probe IDs of differentially expressed genes were converted to their corresponding Ensembl ID and mapped in the *Interferome* database focusing on blood-specific IRG (version 2.01, update of 2015, http://interferome.its.monash.edu.au/interferome/home.jspx) [13,34]. Briefly, all the filtered probes in the transcriptomics datasets were submitted to DAVID gene ID conversion tool [38] to retrieve Ensemble and gene symbol identifiers and isolate the probes relative to IRG. As further control, the same probe list was submitted to biomaRt ID conversion package in R Bioconductor [39].

To verify whether MS B cell or monocyte transcriptomes were enriched in dysregulated IRG, we measured the frequency of differential expression in IRG list and in the global transcriptome as previously described [17], and verified whether the frequency of IRG differentially expressed genes was significantly higher in the IRG list than the expected frequency of dysregulation in a random selection of transcripts from the database by chi-square test with Yates's correction in Graph Pad [13]. Z score was calculated by Z = r-n ((R/N)/Sqrt (n(R/N) (1-R/N) (1-(n-1/N-1)) [40], where R is the number of dysregulated probes in the global transcriptome, N is the total number of expressed probes in the global transcriptome, r is the number of differentially expressed IRG probes and n is the total number of expressed IRG probes.

2.7. Gene ontology and pathway enrichment analysis

Genecodis program [41] was used to search for gene ontology (GO) biological processes and pathways enriched in the gene list and selected those terms passing the p-value threshold of 0.05 and containing at least three differentially expressed genes. The database was annotated with approximately 95% of the genes in our gene list.

2.8. Retro-transcription and quantitative real time PCR

Purified RNA was reverse-transcribed by the Murine Leukaemia Virus Reverse Transcriptase (Invitrogen, Thermo Fisher Scientific). Expression of the genes encoding caspase-3, Interleukin-16 (IL-16), STAT3, myeloid differentiation primary response gene 88 (MyD88), OAS1, IRF1 and 7, AIM2 (absent in melanoma 2 gene), (sp110 nuclear body protein gene) SP110, Mx dynamin-like GTPase 1 (Mx1), IFNAR1 and IFNAR2 was measured by quantitative real time PCR using the appropriate TaqMan™ assay, chosen by matching the Illumina probe ID found dysregulated in the array list, and TaqMan™ Universal Master Mix II (Applied Biosystems, Thermo Fisher Scientific) on a ViiA™ 7 Instrument (Applied Biosystems, Thermo Fisher Scientific).

In EBV-infected cultures quantitative real time PCR analysis was conducted to analyze viral and cellular gene expression as previously described [36,37]. Briefly, expression of the Mx1 gene as well as of the viral transcripts for EBV-encoded small RNA 1 (EBER-1) and the lytic gene BZLF1 were quantified by using the Light Cycler Fast Start DNA SYBR Green I Master Mix (Roche Diagnostics) in the presence of 3 μM $MgCl_2$ on a LightCycler Instrument (Roche Diagnostics) [37].

The housekeeping gene TATA-box-binding protein (TBP), whose expression was proven stable in proliferating and non proliferating cells [36] and by analyzing the array lists of both monocytes and B cells, was used as normalizer.

Real time reactions were run at least in duplicates. Sample values for each mRNA were normalized to the selected housekeeping gene using formula $2^{-\Delta Ct}$.

2.9. Protein preparation and western blotting

Whole cell extracts were prepared as previously described [42]. Briefly, cells (at least 10^6) were lysed in 10 μl/10^6 cells of ice-cold RIPA-modified whole cell extraction buffer [1% Nonidet P-40, 150 mM NaCl,

A.

Exploratory cohort	B cells	Monocytes
RR-MS Number (Female : Male)	25 (17 : 08)	25 (17 : 08)
Median Age ± SD, years	39 ± 1	39 ± 1
HD Number (Female : Male)	24 (15 : 09)	21 (13 : 08)
Median Age ± SD, years	36 ± 7.4	36 ± 7.7

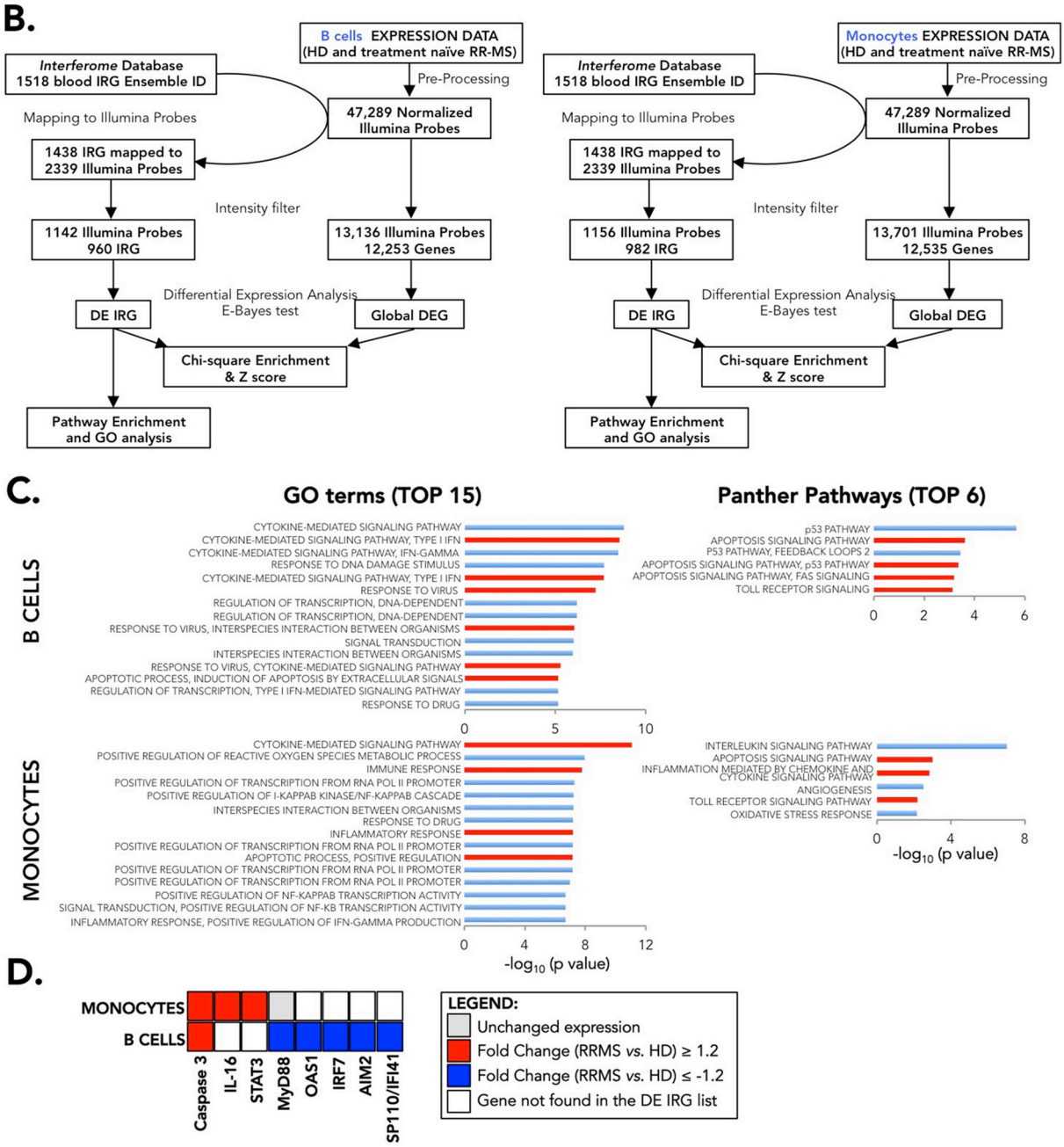

Fig. 1. ***Interferome*-based transcriptome analysis of B cells and monocytes. A.** Summary of demographic characteristics (sex and age) of MS patients and healthy donors (HD) used for transcriptome analysis of B cells and monocytes. **B.** Flow charts for transcriptomics study of B cells and monocytes. DE IRG, differentially expressed IFN-regulated genes in MS patients. DEG, differentially expressed genes. **C.** Top 15 gene ontology (GO) terms and top 6 panther pathways emerged from the analysis of B cell and monocyte transcriptomes graphed by using the formula -$\log_{10}$ of their p-value. In red GO processes and pathways that were further validated. **D.** Gene nodes selected for molecular and functional validation studies. As indicated by a color code, red color indicates gene fold change (RRMS *vs.* HD) equal or greater than 1.2; blue color stands for gene fold change (RRMS *vs.* HD) equal or lower than 1.2. Grey color indicates unchanged expression of the gene in a dataset derived from a specific cell type. White color indicates that gene was not found in the DE IRG list of a specific dataset. (For interpretation of the references to color in this figure legend, the reader is referred to the Web version of this article.)

1 mM EDTA pH = 8, 10% glycerol, 50 mM TRIS buffer pH = 7.4 together with 1 mM PMSF and 1× protease inhibitor cocktail (Sigma Aldrich)].

Western blotting was performed as previously described [43]. Briefly, protein extracts were separated on 15% SDS-PAGE gel and blotted onto nitrocellulose membranes (Millipore). Blots from monocyte extracts were incubated with rabbit anti-STAT3 mAb (C-terminal, Cell Signaling technology, clone 79D7), mouse anti-STAT3 mAb (N-terminal, BD Transduction lab, clone 84/Stat3) or *anti*-IL-16 Ab (R&D Systems, clone Q140005), as needed. Blots from B cells were incubated with Abs anti-STAT1 (BD Transduction Laboratories, clone 42/STAT1) and 2 (BD Transduction Laboratories, clone 22/Stat2) as well as *anti*-phospho-STAT1 (Y701, Cell Signaling, clone D4A7) and 2 (Y689, R&D Systems, clone 1021D). Detection was achieved using anti-rabbit, anti-mouse or anti-goat horseradish peroxidase-conjugate secondary Ab (Santa Cruz Biotechnology) as needed, and visualized with Enhanced Chemiluminescence plus kit (GE Healthcare Bio-Sciences). A ChemiDoc XRS (Bio-Rad) instrument and ImageLab software (Bio-Rad) were used to reveal and analyze the chemiluminescence signal.

For loading control, β-actin levels were quantified by using a goat *anti*-β-actin Ab (Santa Cruz, clone I-19). Protein amount was quantified by Bradford method (Bio-Rad) and normalized to the actin level by ImageLab software (Bio-Rad). To make sure to correctly compare cells from patients to those of HD, each sample was loaded onto gel considering the initial number of lysed cells.

2.10. EBV infection

GFP-transformed EBV (2089 strain) was produced in a cell line (2089/293) based on 293 cells stably transduced with a GFP-encoding recombinant EBV genome based on B95.8 EBV strain [44]. Supernatants containing virus particles were purified by centrifugation of cell debris (300 g, 5 min) and filtration (0.45 μm pore size).

PBMC were infected with 100 μl of viral supernatant/10^6 cells after 1.5 h viral adsorption at 37 °C and then plated at 5 × 10^6 cells/ml in 24-wells plates (Costar). Cells were cultured at the indicated time points in RPMI 1640 (BioWhittaker Europe) supplemented with 2 mM L-glutamine, 100 U/ml penicillin, 100 μg/ml streptomycin (Gibco) and 20% FBS (BioWhittaker Europe) in presence of 1 μg/ml of Cyclosporin A (Sigma-Aldrich) and complete medium was changed once a week.

2.11. In silico analysis of human IL-16 promoter

The *in silico* analysis of the human promoter of the IL-16 gene (accession number NM_001172128.1, full length pro-IL-16 variant 3) was done by using the transcription factor binding site prediction program *MatInspector* (online at www.genomatix.de/matinspector.html) [45]. *MatInspector* analysis was then implemented with gene information contained in the human gene database GeneCards® (online at https://www.genecards.org). Transcription factor binding sites were analyzed in a region spanning 500 bp upstream and 360 bp downstream the transcription starting site (TSS) of the gene. Enhancer elements were also studied revealing an important STAT3 binding site at +154 Kb from the TSS, besides those contained within the classical promoter region. STAT3 binding sites, together with STAT1 (alpha and beta), are considered top transcription factor binding sites within the human IL-16 promoter and those with the highest gene association score (https://www.genecards.org/cgi-bin/carddisp.pl?gene=IL16&keywords=IL-16).

2.12. Statistical analysis

Statistical significance of differences was determined by using Ministat 2.1 software. Student's t-test was used for paired data. For unpaired data, Mann-Whitney *U* test was applied for comparisons between two groups, whereas two-way Anova was utilized for comparisons between more than two groups using two-tailed *p*-values.

Results were shown as median values ± SD. $P \leq 0.05$ was considered significant. In the figures, star scale was assigned as follows: * = $p \leq 0.05$; ** = $p \leq 0.01$; *** = $p \leq 0.001$.

3. Results

3.1. Cell-type specific transcriptomic analysis of interferome in MS

To investigate the cell type-specific expression level of IRG in RRMS, we performed high-throughput transcriptomics profiling of freshly isolated (*ex vivo*) B cells and monocytes from therapy-free RRMS patients and sex- and age-matched HD enrolled within the exploratory cohort (Fig. 1A, Supplementary Tables 1 and 3). Around 13,000 probes were found expressed in B cell and monocyte transcriptomes. The Illumina Probe IDs of expressed transcripts were converted to their corresponding Ensembl ID and mapped in the *Interferome* database focusing on blood-specific IRG (2.01 updated version). Of 1438 IRG genes defined in the *Interferome* database 1142 and 1156 were expressed in B cells and monocytes, respectively (Fig. 1B). The Bayesian analysis identified that 285 and 158 IRG probes were differentially expressed in B cells and monocytes of RRMS patients and HD (Supplementary Tables 5 and 6). Particularly, in RRMS monocytes, the differentially expressed IRG reflected a more pro-inflammatory phenotype of these cells with higher expression of activation markers, such as CD69 and CD86, IFN-γ receptor chain 2 (IFNGR2) and chemokine receptors CCR1 and CCR2, and lower levels of the interleukin-1 receptor antagonist (IL-1RA) as compared to HD cells (see Supplementary Table 6). Similarly, MS B cells expressed higher levels of IFNGR1 and kinases involved in pro-inflammatory cytokine production such as the IL-1 receptor-associated kinase 3 (IRAK3) and TANK binding kinase 1 (TBK1), whereas genes linked to anti-viral responses such as IRF7, OAS1 and OAS3 were strongly down-regulated (see Supplementary Table 5).

To evaluate whether transcriptomes of RRMS B cells and monocytes were enriched in dysregulated IRG, we measured the frequency of differential expression in the list of expressed IRG and in the global transcriptome for each cell type, and calculated whether the frequency of dysregulation of IRG was significantly higher in this list than the expected frequency of differential expression in a random selection of transcripts from the whole transcriptome. As shown in Table 1, the enrichment in dysregulated IRG was significant in both transcriptomes derived from B cells and monocytes of RRMS patients.

GO and pathway analyses participated by the differentially expressed IRG unraveled significant cell type-specific changes in MS (Fig. 1C; Supplementary Tables 7–10). When focusing on the emerged dysregulated terms, we noticed a significant enrichment in genes

Table 1
Probability of enrichment in differentially expressed IFN-regulated genes in B cells and Monocytes of relapsing-remitting multiple sclerosis patients.

Raw p value	DE IRG	All IRG	IRG Frequency (%)	All DEG	Total no. Probes	Global Frequency (%)	Chi square	P Value
B cells	285	1142	24.9	3645	13,136	27.7	4.71	0.03
Monocytes	158	1156	13.6	1616	13,701	11.7	4.06	0.04

IRG, Interferon-regulated genes; DE, differentially expressed; FDR-c, false discovery rate-corrected.

involved in "type I IFN-mediated signaling and response to virus pathways" in B cells and in "inflammation mediated by chemokine and cytokine signaling pathway" in monocytes. Conversely, in both cell types from MS patients, the "apoptotic process" and the "Toll-like receptor (TLR) signaling pathway" were commonly altered. Indeed, several key nodes of these biological processes were dysregulated at transcriptional level. Some were found altered in both MS B cells and monocytes, as the gene encoding caspase-3, considered the effector enzyme for execution of apoptotic cell death [46] (Fig. 1D). Other genes like the transcription factor STAT3, which regulates expression of many

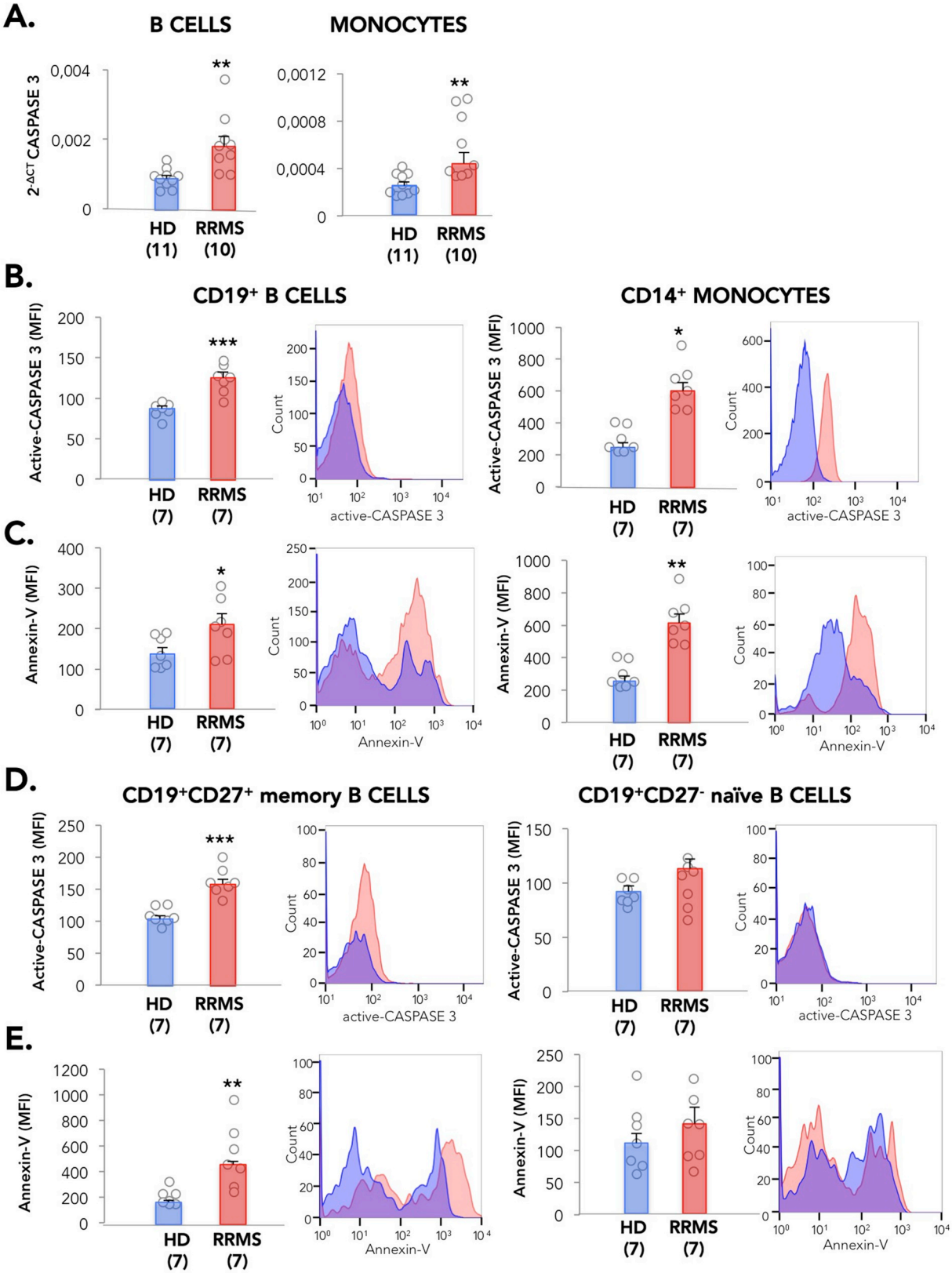

(caption on next page)

Fig. 2. Analysis of apoptotic pathway in B cells and monocytes. A. Quantitative real time PCR of caspase-3 gene expression in freshly isolated paired B cells (**p = 0.007) and monocytes (**p = 0.009) from 10 RRMS patients (red bars) and 11 matched HD (blue bars) enrolled in the validation cohort. mRNA level of expression was normalized to TBP using formula $2^{-\Delta Ct}$. Error bars show median values ± SD. Each dot represents a single RRMS patient or HD. **B-C.** Intracellular active caspase-3 (B) and surface Annexin-V (C) level of expression were measured by flow cytometry in gated $CD19^+$ B cells and $CD14^+$ monocytes in PBMC of 7 RRMS patients and 7 matched HD. For caspase-3: ***p (B cells) = 0.0001; *p (monocytes) = 0.019. For Annexin-V: *p (B cells) = 0.03; **p (monocytes) = 0.0016. **D-E.** Intracellular active caspase-3 (D) and surface Annexin-V (E) were also studied in gated $CD19^+CD27^+$ memory and $CD19^+CD27^-$ naïve B cells. For caspase-3: ***p($CD19^+CD27^+$) = 0.0001. For Annexin-V: **p($CD19^+CD27^+$) = 0.003. Values of mean fluorescence intensity (MFI) are depicted for each studied individual, together with median ± SD values. For each experimental condition representative flow cytometry histograms are included. (For interpretation of the references to color in this figure legend, the reader is referred to the Web version of this article.)

cytokines [47], and IL-16, a chemokine for $CD4^+$ T cells [48], were exclusively dysregulated in MS monocytes. Instead, in MS B cells, the predominant gene expression changes noted were in the type I IFN inducible genes encoding for proteins involved in anti-viral responses, like OAS1, IRF7 [49], absent in melanoma 2 gene, AIM2 [50] and SP110/IFN inducible protein (IFI) 41 or IFI75 [51] and MyD88, a key adaptor protein involved in TLR signaling [52] (Fig. 1D). These genes were selected for in-depth validation studies on newly isolated monocytes and B cells from a second independent case-control cohort of RRMS patients and matched HD (see Supplementary Tables 2 and 4).

3.2. "Apoptotic signaling pathway" in MS B cells and monocytes

Among different components of the apoptotic process dysregulated in either B cells or monocytes, the *Interferome*-filtered analysis of transcriptomes highlighted up-regulation of the pro-apoptotic caspase-3, tyrosin kinase LYN and FAS receptor, and down-regulation of the anti-apoptotic protein of the BCL-2 family MCL1 (Supplementary Tables 5 and 6).

We validated higher expression of caspase-3 gene detected by quantitative real time PCR (Fig. 2A) and stronger activation of intracellular caspase-3 protein by flow cytometry (Fig. 2B) in both monocytes and B cells of patients in comparison to HD. Accordingly, an increased binding of Annexin-V to phosphatidylserine on the outer leaflet of the apoptotic cell plasma membrane was found in MS B cells and monocytes, further confirming a critical alteration of this cellular state in MS (Fig. 2C). The distinct characterization of $CD27^-$ (naïve) and $CD27^+$ (memory) B cells, gated as in Supplementary Fig. 1, showed that mainly memory B cells displayed an apoptotic phenotype in MS (as seen for both caspase-3 activation and Annexin-V expression) (Fig. 2D and E).

These findings underline apoptosis as common active trait in MS monocytes and B cells.

3.3. "Inflammation mediated by chemokine and cytokine signaling pathway" in MS monocytes

Our *Interferome*-based study revealed a MS-associated monocyte-specific dysregulation in genes involved in "immune response" and "cytokine-mediated signaling pathways". In particular, one of the top up-regulated genes in MS monocytes encoding IL-16, a chemoattractant and activator of $CD4^+$ T cells (see Supplementary Tables 8 and 10) drew our attention and was further examined. We first quantified its expression by real time PCR in samples derived from the validation cohort and confirmed a specific and statistically significant IL-16 up-regulation in MS monocytes and not in B cells (Fig. 3A). *In silico* analysis of the human IL-16 gene tracked down the main transcription factors involved in the regulation of its expression and highlighted several STAT3 binding sites within the promoter region and in an enhancer element downstream the starting site of the IL-16 gene (Fig. 3B). Interestingly, STAT3 gene was one of the differentially expressed IRG in MS monocytes (see Supplementary Tables 8 and 10) and was validated by quantitative PCR in the second independent cohort (Fig. 3C). It is known that the main STAT3 isoforms differ by a few amino acids with a molecular weight ranging from 88 to 83 kDa, due to proteolytic processing at the C-terminus of the protein. Instead, the presence of multiple cleavage sites for active caspase-3 at the N-terminus leads to fragments ranging from 70 to 50 kDa [53]. Western blotting analysis with Abs directed to the C- or N-terminus of STAT3 confirmed higher level of STAT3 protein in *ex vivo* monocyte lysates derived from RRMS patients than in sex- and age-matched HD (Fig. 3D). Importantly, the N-terminal pattern was more consistently characterized by cleaved STAT3 bands in MS monocytes (Fig. 3D), demonstrating enhanced activity of caspase-3 *in vivo*.

Considering that the primary transcript of IL-16, encoding the pro-IL-16 form (45 kDa), is also cleaved into a short bioactive form of 15 kDa by active caspase-3 that can be then released from the cells [54], we verified the state of IL-16 protein *ex vivo* and *in vitro* in MS and healthy monocytes. This experiment unraveled higher levels of pro-IL-16 in MS cells than in controls (Fig. 3E). This is consistent with quantitative real time PCR data. Moreover, we detected more abundant active IL-16 in MS monocytes compared to HD cells when cultured in presence of the protein transport inhibitor GolgiPlug™, suggesting that the higher activity of caspase-3 in MS monocytes induces the cleavage of IL-16 into the active released form, akin to that observed in HD cells upon treatment with Staurosporine, a chemical caspase-3 activator (Fig. 3E). Indeed, inhibition of caspase-3 completely blocked IL-16 cleavage in cultures of MS monocytes (Fig. 3F). Overall these experiments demonstrate that, in addition to cell fate, ongoing apoptosis in MS immune cells may determine cell function via induction of STAT3 and production of IL-16.

3.4. "Type I IFN-mediated signaling" and "response to virus" pathways in MS B cells

Intriguing data point to the association of MS with EBV, a herpesvirus with B cells as its latent reservoir [5]. Interestingly, our cell type-specific *Interferome*-based transcriptomics analysis indicated the down-regulation of several genes involved in "type I IFN-mediated signaling and response to virus pathways" specifically in B cells of RRMS patients, e.g. IRF7, OAS1, SP110, AIM2, MyD88 and others (see Supplementary Tables 7 and 9). Validation studies confirmed that transcripts of selected IRG were dramatically decreased in B cells of MS patients as compared to HD, while unchanged in monocytes (Fig. 4A). Furthermore, the responsiveness to increasing low doses of recombinant type I IFNs, which trigger the antiviral responses, was found strongly depressed in MS B cells, as demonstrated by the levels of the classical type I IFN inducible gene Mx1 (Fig. 4B). Conversely, no significant difference in IFN-γ-mediated induction of IRF1 was detected in the cells of RRMS patients and HD (Fig. 4C). Thus, MS B cells display a specific alteration of the type I IFN signaling pathway at multiple levels. Accordingly, the transcription of both type I IFN receptor IFNAR1 and 2 chains was significantly lower in MS B cells than in controls and, notably, was restored upon *in vivo* IFN-β treatment (Fig. 5A). Surface expression of IFNAR1 and IFNAR2 proteins, monitored by flow cytometry, dropped in terms of intensity of expression and frequency in $CD19^+$ B cells of MS patients in comparison to HD (Fig. 5B and Supplementary Figs. 2A–B). This decrease affected both $CD27^+$ memory and $CD27^-$ naïve B cell subsets, although a major impact was found in the memory compartment (Fig. 5B and Supplementary Figs. 2A–B). Conversely, no difference in the expression of type I IFN receptors was observed in $CD3^+$ T cells and $CD14^+$ monocytes between

MS patients and HD (Supplementary Fig. 2C). Finally, the basal and IFN-β-induced phosphorylation of STAT1 and 2, two transcription factors necessary for IFN-regulated transcription, was much lower in MS B lymphocytes than in healthy counterparts (Fig. 5C), further demonstrating an overall weak type I IFN signaling in MS B cells.

To verify the functional impact of these alterations on the antiviral response of MS B cells, we infected PBMC from 3 RRMS patients and 3 matched HD with a GFP-transformed EBV strain (2089) in presence of Cyclosporin A, and measured the efficiency of EBV infection by monitoring the frequency of GFP-positive cells at distinct time points up to

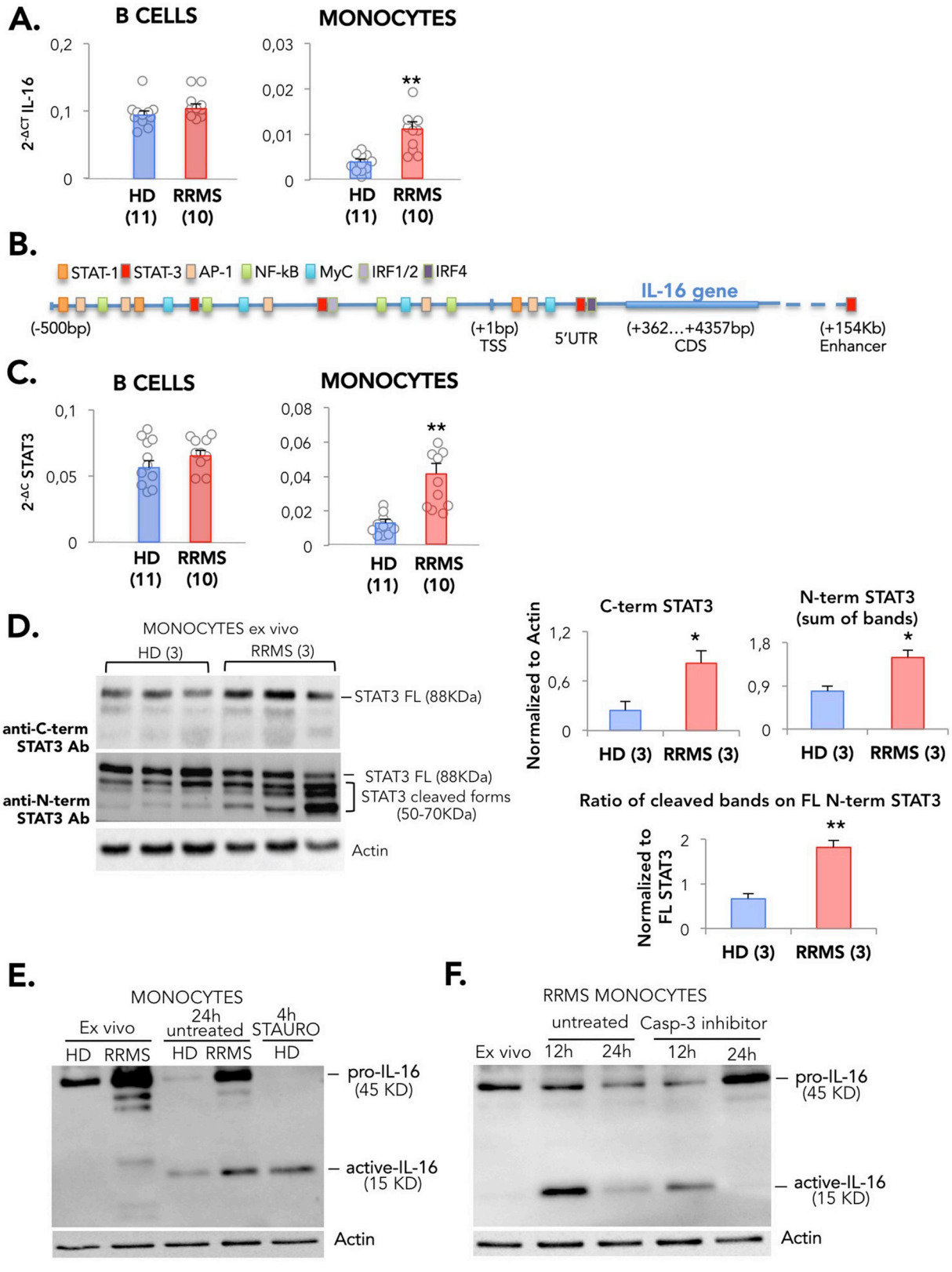

(caption on next page)

Fig. 3. Characterization of IL-16/STAT3 axis in monocytes. A. Expression level of IL-16 gene was evaluated by real-time PCR in freshly isolated B cells and monocytes (**p = 0.002) from 10 RRMS patients (red bars) and 11 matched HD (blue bars) enrolled in the validation cohort. mRNA level of IL-16 gene was normalized to TBP using formula $2^{-\Delta Ct}$. Error bars show median values ± SD. Each dot represents a single RRMS patient or HD. **B.** Schematic map of *in silico* analysis of human IL-16 promoter and enhancer element showing the main transcription factors and their binding sites involved in IL-16 gene transcription. TSS, transcription start site; UTR, untranslated region; CDS, coding sequence; bp, base pair, Kb, kilobases. **C.** Quantitative real time PCR of STAT3 gene expression was performed in freshly isolated B cells and monocytes (**p = 0.002) as in A. **D.** Protein lysates were prepared from freshly isolated (*ex vivo)* monocytes of 3 RRMS and 3 matched HD. STAT3 full length (FL, 88 kDa) expression was analyzed by western blotting by using an *anti*-C-terminal STAT3 Ab. STAT3 caspase-3-cleaved forms (ranging from 70 to 50 KDa) were detected by using an *anti*-N-terminal STAT3 Ab. Signals derived from C-terminal STAT3 FL and N-terminal STAT3 FL and STAT3 cleaved forms were singularly normalized to actin level, used as loading control. Normalized values derived from each HD or RRMS patient were then summed up and median ± SD values derived from 3 HD and 3 RRMS were graphed. *p (C-terminal STAT3) = 0.03; *p (N-terminal STAT3) = 0.04. Signals derived from STAT3 cleaved forms were also normalized on N-terminal STAT3 FL (**p = 0.01). **E.** Protein lysates were prepared from monocytes of HD or RRMS *ex vivo* or left untreated in culture for 24 h (h). As positive control, monocytes from HD were also treated for 4 h with the caspase-3 activator Staurosporine (STAURO) in presence of the protein transport inhibitor Golgi plug*. Pro-IL16 (45 kDa) as well as the cleaved active IL-16 form (15 kDa) were detected by western blotting by using a polyclonal *anti*-IL16 Ab. Results are representative of experiments conducted on cells of 3 different HD or RRMS individuals. **F.** Monocytes were isolated from a RRMS patient and protein extracts were prepared from freshly isolated cells or cells left untreated or treated with a caspase-3 inhibitor for 12 and 24 h. Results are representative of experiments conducted on 3 different HD or RRMS individuals. As loading control, actin level was assayed on all samples (E, F). (For interpretation of the references to color in this figure legend, the reader is referred to the Web version of this article.)

14 days of culture. In this experimental setting we found significantly higher EBV infection in MS B cells at the final timepoint (Fig. 6A). These data were in line with the increased proliferation of $CD19^+$ B cells (Fig. 6B), greater differentiation into $CD38^+CD138^+$ plasmablasts (Fig. 6C), higher expression of the viral transcripts EBER-1, a small non-coding RNA expressed in all phases of latency, and BZLF1, responsible for the activation of lytic/replication cycle [55], in MS patients as compared to HD (Fig. 6D).

As expected, no effect on EBV infection was observed in cultures from HD pre-treated cells with recombinant IFN-β (Fig. 6A–D), demonstrating an ongoing anti-viral response induced by the endogenous type I IFN production upon EBV challenge. Conversely, exposure of MS cells to IFN-β dramatically decreased the frequency of EBV-GFP-positive cells and their ability to proliferate upon EBV infection (Fig. 6A–D). Mx1 expression was induced by IFN-β in HD cultures in the first hours of treatment and then declined as expected (Fig. 6D, lowest panel, blue line). Differently, its induction was weaker in IFN-β-treated MS cells than in HD but subsequently increased at day 3, reaching a higher and more sustained levels than in the HD counterpart until day 7 (Fig. 6D, lowest panel, red line). This is likely due to the capacity of IFN-β to potentiate the type I IFN signaling machinery to contain EBV infection in MS B cells to the level found in HD and to induce the generally deficient antiviral responses. Consistent with this view and with a subsequent induction of Mx1, IFN-β pre-treatment was able to strongly induce both IFNAR1 and IFNAR2 upon 3 days of treatment only in MS cultures (Fig. 6E).

Overall, the *Interferome* analysis followed by functional validation unveiled a breakdown in the endogenous type I IFN-mediated signaling pathway and antiviral responses specifically in B cells of MS patients, with potential consequences on the containment of EBV infection.

4. Discussion

In this study we provide evidence for a pathogenic contribution of altered IFN-regulated genes and pathways in B cell and monocyte immune responses in MS. The comprehensive molecular and functional analysis of selected dysregulated IRG, intracellular cascades and cell functions highlighted: 1) the ongoing caspase-3 dependent apoptotic cell death in MS B lymphocytes and monocytes that may arise from their continuous engagement in MS pro-inflammatory responses; 2) the significant induction of the STAT3/IL-16 axis in MS monocytes, possibly influencing migration of inflammatory $CD4^+$ T cells; 3) the widespread impairment of IFN receptors, transcription factors and protein adapters, involved in type I IFN-mediated signaling in MS B cells; 4) the defective control of EBV infection in MS B cells, which is partly recovered by the treatment with IFN-β.

The perturbation of the constitutive “tonic” production of IFN has been linked to the development of a number of different diseases, including systemic lupus erythematosus, Sjögren's syndrome, or type I diabetes mellitus, often correlating with increased disease severity [56–58]. Accordingly, most MS patients have low levels of serum IFN than healthy counterparts [59] and, during MS exacerbations and active clinical progression, cultured PBMC are resistant to IFN-β treatment and need higher doses to trigger a response, suggesting an endogenous, state-dependent defect of IFN signaling in MS [60].

Interferome is an on-line open access database with a compilation of microarray datasets derived from various cell types and tissues stimulated with type I, II and III IFNs that enables a comprehensive vision of IFN-regulated cell processes and pathways facilitating the systems biology of IFN response [33,34]. By taking advantage of the full access to this database, we performed microarray profiling of unmanipulated, freshly isolated B cells and monocytes from therapy-free patients and matched HD to identify immune cell-specific MS-associated changes in IRG.

In particular, *Interferome*-filtered transcriptome analysis identified altered expression in MS cells of many previously uncharacterized IRG with known immunological functions and defined specific features of these cell types associated to disease. An activated phenotype emerged for both B cells and monocytes of therapy-naïve MS patients as compared to healthy cells. The MS monocytes display higher expression, among others, of the activation markers CD69 and CD86, of the chemokine receptors CCR1 and CCR2 and IFNGR2. Similarly, the MS B cells expressed higher levels of IFNGR1 but also of kinases involved in pro-inflammatory cytokine production such as IRAK3 and TBK1. Dysregulation in protein expression of some of these molecules has been previously shown in MS mainly on T cells. Furthermore, their alterations have also been reported in B cells and monocytes, in longitudinal studies conducted in patients before and after therapy administration or at different stages of the disease [61–69].

Pathway analysis of dysregulated *Interferome* highlighted apoptosis, which regulates survival/death balance of activated lymphocytes and is, thus, considered crucial for the evolution of MS disease [70], as candidate process governing cell fate of both MS B cells and monocytes. Both extrinsic and intrinsic apoptotic pathways converge to the cleavage of pro-caspase-3 into its mature active form [71]. A number of studies investigating this process in MS blood cells showed lower susceptibility of PBMC from RRMS and secondary progressive MS patients to cell death [72] and defective caspase-3 activation and apoptosis in T lymphocytes of RRMS [73] and primary progressive MS [74] patients. In contrast, our study identified higher caspase-3 expression and activation as well as increased Annexin-V levels in B cells and monocytes of MS patients as compared to the healthy counterparts. This novel observation in antigen-presenting cells of MS patients might be the consequence of immune cell exhaustion due to chronic activation. Indeed, MHC class II protein expression is enhanced in both MS B cells [75] and monocytes [76], indicating a continued stimulation, which in turn

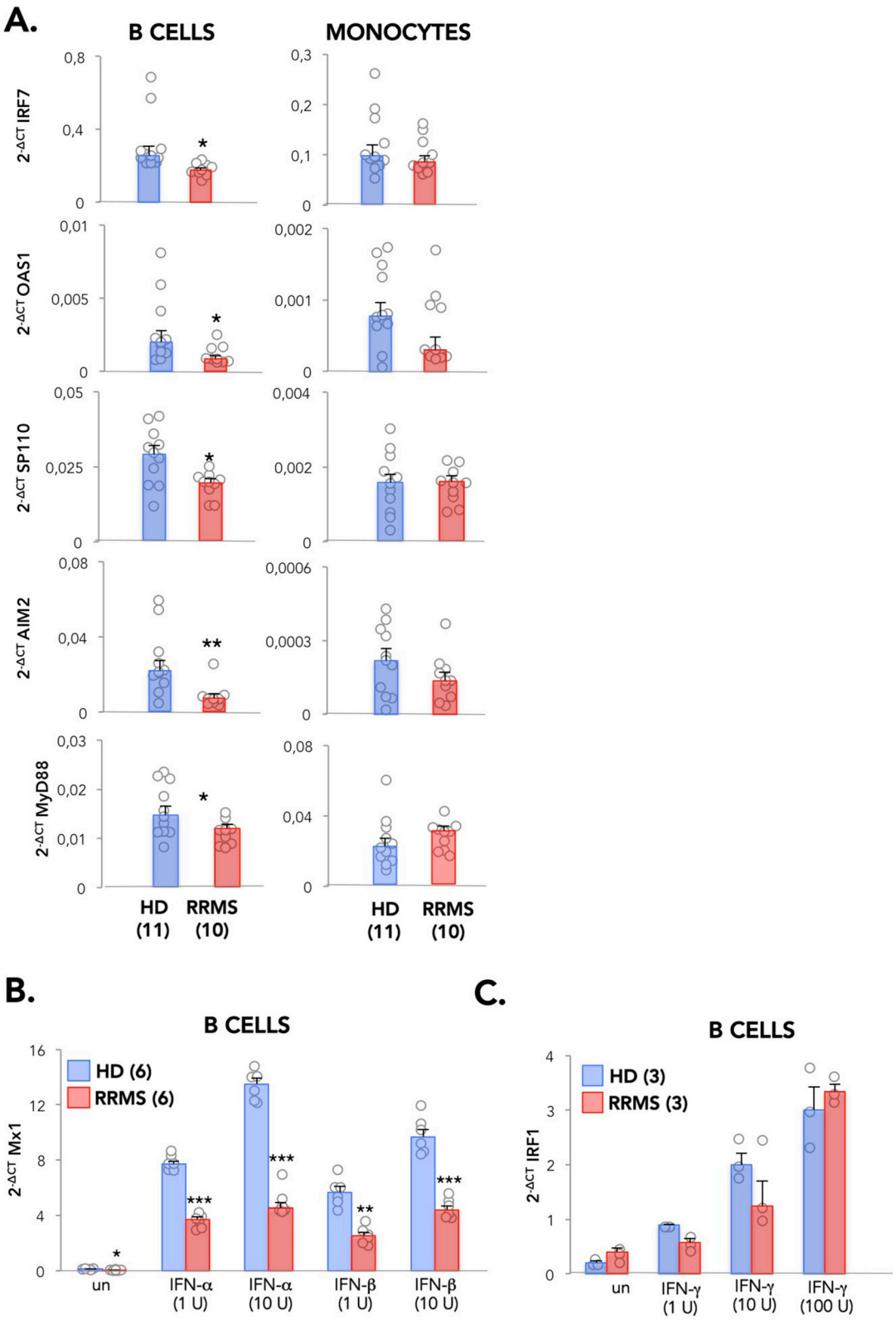

Fig. 4. Characterization of type I IFN-mediated signaling and response to virus pathways in B cells. A. Quantitative real time PCR of selected differentially expressed IFN-regulated genes was performed in freshly isolated B cells and monocytes from 10 RRMS patients (red bars) and 11 matched HD (blue bars) enrolled in the validation cohort. mRNA level of expression was normalized to TBP using formula $2^{-\Delta Ct}$. Error bars show median values ± SD. Each dot represents a single RRMS patient or HD. For B cells: IRF7, *p = 0.02; OAS1, *p = 0.027; SP110, *p = 0.018; AIM2, **p = 0.001; MYD88, *p = 0.03. **B.** Mx1 gene expression was quantified as in (A) in B cells from 6 HD and 6 RRMS from validation cohort treated for 1 h with 1 and 10 units/ml (U) of IFN-α or IFN-β. P values were calculated comparing the same experimental condition in RRMS or HD cells. Untreated (un), *p = 0.02; 1U IFN-α, ***p = 8E-05; 10U IFN-α, ***p = 3.6E-05; 1U IFN-β, **p = 0.006; 10U IFN-β, ***p = 0.001. **C.** Quantitative gene expression for IRF1 was conducted as in (B) in B cells from 3 HD and 3 RRMS from validation cohort treated for 1 h with 1, 10 and 100 units/ml (U) of IFN-γ. (For interpretation of the references to color in this figure legend, the reader is referred to the Web version of this article.)

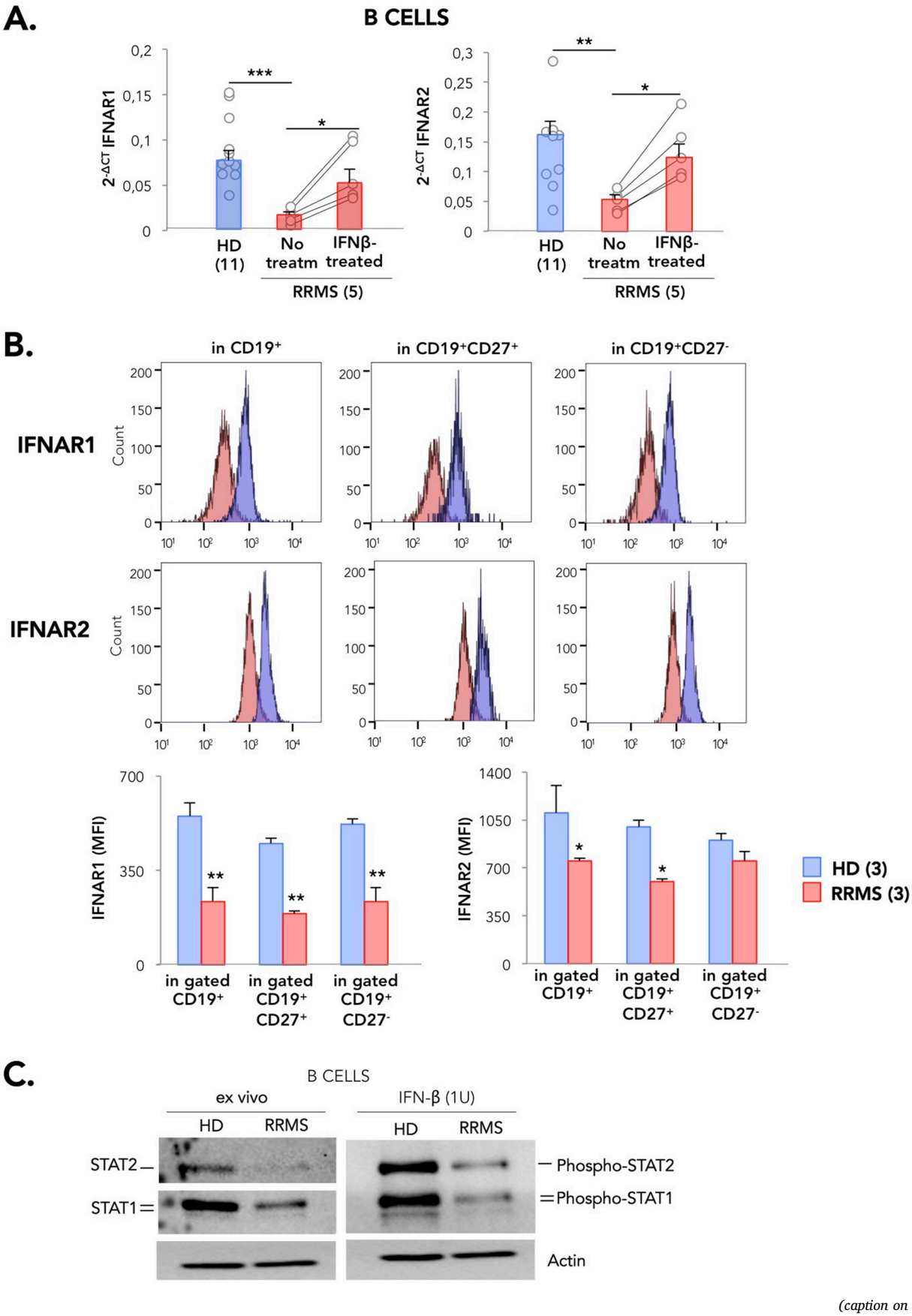

(caption on next page)

Fig. 5. Type I IFN intracellular signaling is depressed in B cells of RRMS patients. A. Quantitative real time PCR of IFNAR1 and IFNAR2 genes was performed in freshly isolated B cells from 11 HD (blue bars) and 5 RRMS patients (red bars) longitudinally sampled before (No treatm) and one month after the beginning of *in vivo* IFN-β therapy (IFN-β-treated). mRNA level of expression was normalized to TBP using formula $2^{-\Delta Ct}$. Error bars show median values ± SD. Each dot represents a single RRMS patient or HD. For IFNAR1: RRMS (No treatm) vs. HD, ***p = 0.0001; RRMS (No treatm) *vs.* (IFN-β-treated), *p = 0.04. For IFNAR2: RRMS (No treatm) vs. HD, **p = 0.005; RRMS (No treatm) *vs.* (IFN-β-treated), *p = 0.03. **B.** IFNAR1 and IFNAR2 surface expression was studied by flow cytometry in $CD19^+$ B cells, as well as in $CD27^+$ memory and $CD27^-$ naïve B cells gated in $CD19^+$ total B cells from 3 RRMS and 3 matched HD. For each experimental condition representative histograms are shown. Median values ± SD of mean fluorescence intensity (MFI) are depicted for each cell subset analyzed (lower panels). For IFNAR1: **p($CD19^+$; $CD19^+CD27^+$; $CD19^+CD27^-$) = 0.003. For IFNAR2: *p($CD19^+$; $CD19^+CD27^+$) = 0.03. **C.** Protein lysates of 4 RRMS and 4 matched HD were prepared from B cells freshly isolated (*ex vivo)* or treated for 1 h with 1 unit/ml (U) of IFN-β. STAT1 and STAT2 content or phosphorylated forms were detected by western blotting by using the specific Abs. Depicted results are representative of all the experiments performed. As loading control, actin level was assayed on all samples. (For interpretation of the references to color in this figure legend, the reader is referred to the Web version of this article.)

might sustain apoptosis-induced cell death following persistent MHC II ligation by activated T cells [77]. In accordance with this view, we found that apoptosis of MS B cells affected mainly the $CD27^+$ memory compartment, which is considered the most inflammatory and pathogenic B cell subset in MS [24]. Importantly, IFN-β therapy of MS decreases the frequency of circulating $CD27^+$ B cells via FAS-mediated programmed cell death [37], indicating that IFN signaling may exacerbate apoptosis of MS B cells.

Our *Interferome*-based transcriptome study revealed also monocyte-specific alterations in genes involved in "immune response" and "inflammation mediated by chemokine and cytokine signaling pathway", consistent with the view that circulating monocytes expressing high levels of co-stimulatory molecules and pro-inflammatory cytokines stimulate and sustain differentiation of Th-1/Th-17 cells, key drivers of inflammation during MS [78], and are among the first cells to arrive to the brain, together with T lymphocytes, where they initiate and perpetuate inflammation [25]. One of top up-regulated transcripts in MS monocytes was that encoding IL-16, a chemotactic factor specific for $CD4^+$ T lymphocytes [79] that regulates T cell activation and crosstalk with dendritic cells and B cells [79,80]. While it is known that the chemokine IL-16 is widely expressed in cells of peripheral blood [81] and its circulating levels are elevated in untreated RRMS patients and decreased after IFN-β therapy [82]; here we show that monocytes may represent a more robust source of IL-16 transcript and protein in MS than in the healthy condition. IL-16 has been extensively studied both in MS and experimental models [48]. Its expression was found in immune cells infiltrating MS lesions, in particular $CD4^+$ and $CD8^+$ T cells, $CD83^+$ dendritic cells and B cells [83]. IL-16 is generated from a full-length precursor molecule of 80 KDa, the so-called pro-IL-16, which is cleaved at the C-terminal portion into a secreted bioactive form of 17 kDa by active caspase-3 [84]. Interestingly, increased levels of active caspase-3 in RRMS lesions correlate with those of bioactive IL-16 [83,85]. Further, correlation between elevated IL-16 CNS levels and intensity of $CD4^+$ T cell infiltration was demonstrated in RRMS and experimental autoimmune encephalomyelitis suggesting an important role for this chemokine in the regulation of $CD4^+$ T cell infiltration [83,85,86]. Further, we found that STAT3, one of the main IL-16 transcriptional regulators emerged by our *in silico* analysis, is over-expressed at both transcript and protein levels in MS monocytes but not in B cells. Importantly, we provide evidence for caspase-3-mediated cleavage at the N-terminus of STAT3, strongly impacting on the repertoire of STAT3 isoforms in MS monocytes. This pattern was previously described under apoptotic conditions and it is associated with STAT3 translocation into the nucleus and transcription of target genes independently of STAT3 phosphorylation [53]. Besides targeting STAT3, active caspase-3 also enhanced IL-16 cleavage into its bioactive shorter form in MS monocytes. Overall, these data support the hypothesis that chronic peripheral inflammation activates caspase-3-dependent mechanisms in MS monocytes which, while predisposing them to apoptotic cell death, further trigger and perpetuate $CD4^+$ T cell activation and migration into the CNS via IL-16 release.

The *Interferome*-based analysis of B cell transcriptomes revealed that several components of the "type I IFN-mediated signaling and response to virus pathways" were dramatically and specifically impaired in MS B cells. Our study describes for the first time that the expression of several IFN-inducible genes strictly involved in antiviral responses, such as IRF7, SP110, OAS1, and AIM2, showed a strong reduction in MS B cells compared to their counterparts derived from HD. Interestingly, also MyD88 level was reduced suggesting an impaired TLR signaling, while we previously reported that TLR7 and 9 expression is unchanged in MS B cells [32]. When dissecting the type I IFN pathway, we observed an even more profound defect. In fact, MS B cells displayed low transcript and protein levels of IFNAR1 and IFNAR2, weak expression and activation of STAT1 and 2, and selective impairment in responses to type I but not type II IFN. Thus, to the best of our knowledge, our findings for the first time reveal a profound multi-level defect in type I IFN signaling and response to virus pathways in these cells.

Keeping in mind the recent success of B cell-depleting therapies in reducing disease activity and relapse rate in MS [23,87], we hypothesized that these treatments may display antiviral effects by targeting the pathogenic pro-inflammatory memory B cell subset [24], which also represent the EBV reservoir in humans.

The contribution of EBV to MS pathogenesis is still being fervently debated, however several hypotheses have been proposed in support of either a direct or an indirect involvement of this virus in MS [6,88]. In line with this view and with our results pointing to an anti-viral failure in MS B cells, we further investigated whether these cells may display altered viral expression program and virus propagation. Following *in vitro* infection of PBMC with a GFP-transformed EBV strain, stronger expression of the viral transcripts EBER-1 and BZLF1 appeared in MS B cells than in healthy cell cultures. In particular, the immediate early switch gene BZLF1 marking the beginning of the lytic cycle in plasmablasts/plasmacells [89] increased in HD cultures after 14 days of *in vitro* infection. Conversely, its level was induced early and very high in MS cultures, indicating a strong dysregulation in the control of viral cycle by B cells of MS patients. Notably, we provide evidence that, at least in the early phases of *in vitro* infection, EBV propagated more efficiently in MS cultures than in controls. Thus, dysregulation of type I signaling machinery observed in MS B cells may result in reduced containment of EBV infection. This is consistent with the increased EBV gene expression in both peripheral blood and CNS tissues of MS patients reported by others and us [37,90,91] and with more general data showing the pathogenic relevance of the interaction between a MS-predisposing genotype and EBV [92].

The current research adds novel findings in support of those previous studies and may have important implications with regard to the diffusion and maintenance of active EBV infection in MS B cells. Importantly, exposure to IFN-β could potentiate type I IFN signaling machinery in MS as it enhanced IFNAR1 and 2 transcription in B cells *in vitro* and *in vivo* and induced delayed but sustained Mx1 expression in MS B cells *in vitro*. These evidences are in agreement with previous data showing a deficient IFNAR/TLR7 signaling in MS B cells that could be partially rescued by exogenous IFN-β [93]. Finally, we show that *in vitro* exposure to IFN-β, most probably through the induction of the deficient IFN machinery and, in turn, activating the anti-viral responses, reduces the frequency of EBV-infected cells and proliferating B cells in MS but not HD cultures. Significantly, this recapitulates the strong decrease of $CD27^+$ memory B cells and EBV gene expression in peripheral blood of

patients undergoing IFN-β therapy, previously shown by us [37].

Our study profiled changes in IRG associated with MS B cells and monocytes and unveiled novel dysregulation in endogenous IFN signaling and IFN-regulated cell processes specific of these immune subsets, including support of T cell activation and migration via the STAT3/IL-16 axis in monocytes and improper control of EBV infection by B cells.

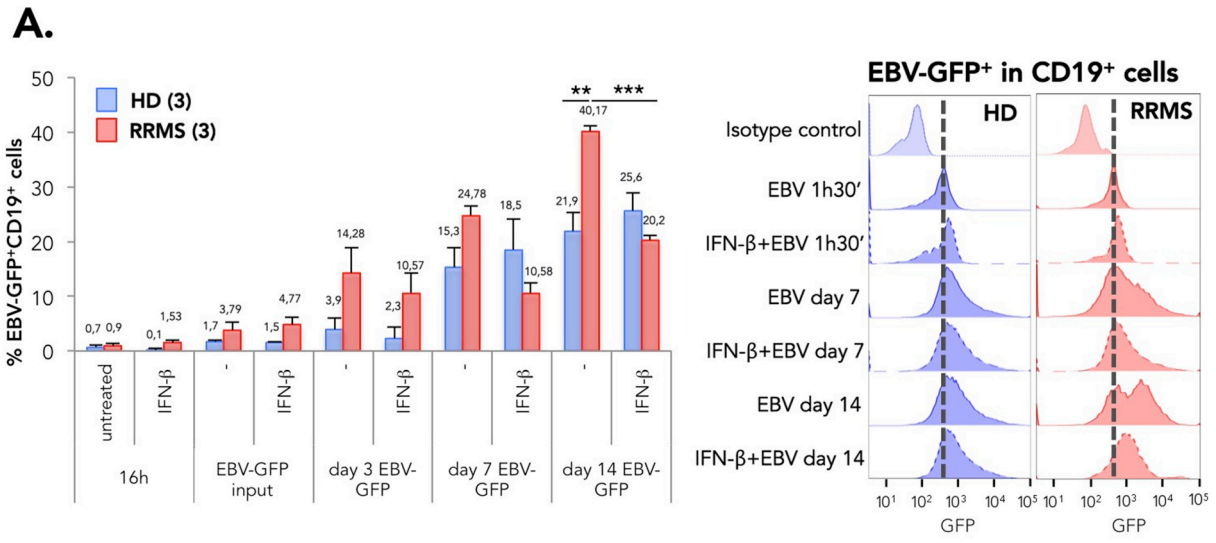

B.

% CD19+ Blasts	HD (3)	RRMS (3)
EBV day 7	18,27±2,1	23,65±10
IFN-β+EBV day 7	12,8±1,5	9,56±3,2*
EBV day 14	22,92±0,9	39,91±5,9*
IFN-β+EBV day 14	21,72±1	15,25±2*

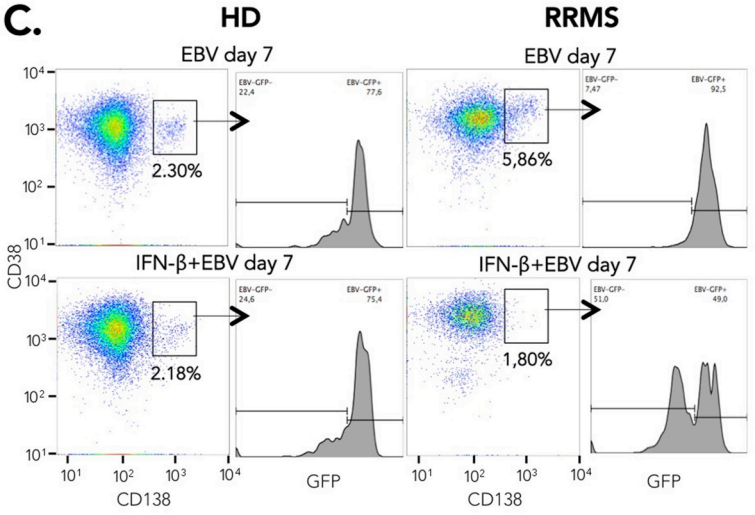

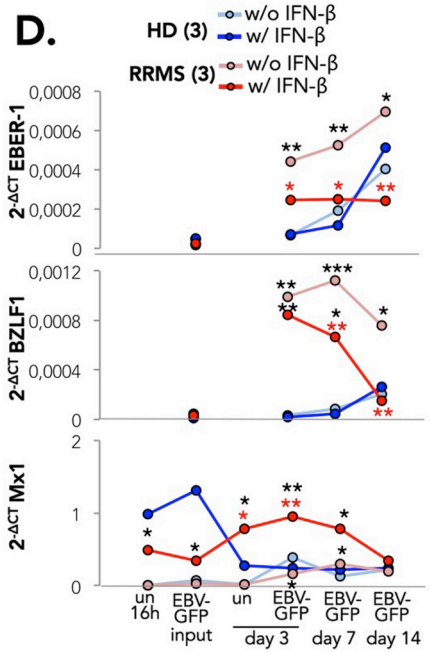

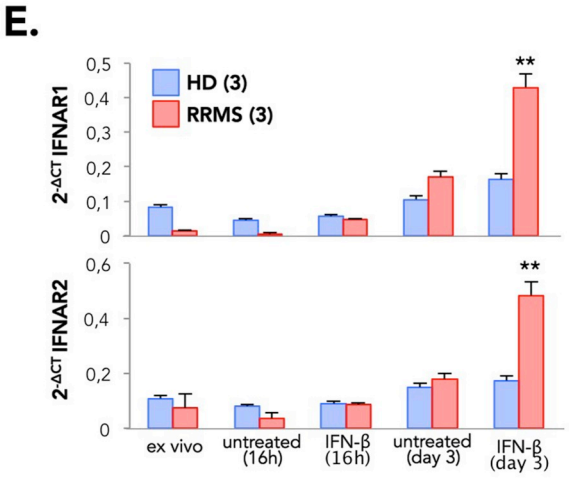

(caption on next page)

Fig. 6. Antiviral response is less effective in B cells of RRMS patients. A-B. PBMC from 3 RRMS patients and 3 matched HD enrolled in the validation cohort were infected with EBV-GFP (2089 strain) in presence or absence of a 16 h pre-treatment with IFN-β (10 units/ml). Then, viral adsorption was conducted for 1.5 h (considered the input signal) in cells untreated or pre-treated with IFN-β. Upon adsorption, cells were left in culture for the indicated time points up to 14 days. **A.** EBV infection was monitored by flow cytometry in gated $CD19^+$ B cells and graphed as median values ± SD of percentage (%) of EBV-GFP^+ cells. RRMS (EBV-GFP day 14) *vs.* HD (EBV-GFP day 14), **p = 0.01; RRMS (EBV-GFP day 14) *vs.* RRMS (EBV-GFP + IFN-β day 14), ***p = 0.001. For each experimental condition graphed in (A), representative flow cytometry histograms derived from 1 RRMS patient and 1 matched HD are shown. **B.** Median values ± SD of % of $CD19^+$ proliferating blasts are reported for day 7 and day 14 of culture in presence or absence of 10 units/ml of IFN-β. P values were calculated comparing the same experimental condition in RRMS or HD cells (black stars), *p (EBV-GFP day 14) = 0.03; or comparing cells of RRMS patients before or after IFN-β pre-treatment (red stars), for IFN-β + EBV-GFP day7 and IFN-β + EBV-GFP day14 *p = 0.03. **C.** Frequency of $CD19^+CD38^+CD138^+$ plasmablasts, and the respective quote of EBV-GFP^+ cells, was evaluated by flow cytometry in Fixable Viability dye negative live cells. Representative dot plots derived from 1 RRMS patient and 1 HD out of 3 analyzed are depicted. **D-E.** Expression level of the EBV transcripts EBER-1 and BZLF1 (D), and of the cellular transcripts Mx1 (D), IFNAR1 and IFNAR2 (E) were measured by quantitative real time PCR in PBMC treated at the indicated time points and experimental conditions. mRNA level of expression was normalized to TBP using formula $2^{-\Delta Ct}$. Error bars show median values obtained from 3 RRMS and 3 HD ± SD. P values were calculated comparing the same experimental condition in RRMS or HD cells (black stars). For EBER-1: EBV-GFP day3, EBV-GFP day7, **p = 0.01; EBV-GFP day14, *p = 0.03. For BZLF1: EBV-GFP day3, IFN-β + EBV-GFP day3, **p = 0.009; EBV-GFP day7, ***p = 0.001; IFN-β + EBV-GFP day7, EBV-GFP day 14, *p = 0.04. For Mx1: IFN-β 16 h, IFN-β + EBV-GFP 1.5 h, IFN-β day3, *p = 0.04; IFN-β + EBV-GFP day3, **p = 0.01; EBV-GFP day 3, EBV-GFP day 7, *p = 0.02. For IFNAR1 and IFNAR2: IFN-β day3, **p = 0.01. In cells of RRMS patients the decrement in gene expression observed in presence of IFN-β pre-treatment was significant in the following experimental conditions (red stars). For EBER-1: IFN-β + EBV-GFP day3, IFN-β + EBV-GFP day 7, *p = 0.04; IFN-β + EBV-GFP day 14, **p = 0.01. For BZLF1: IFN-β + EBV-GFP day 7, IFN-β + EBV-GFP day 14, **p = 0.01. For Mx1: IFN-β day3, p = 0.04; IFN-β + EBV-GFP day3, **p = 0.01. Untreated (un). Without IFN-β pre-treatment (w/o IFN-β); with IFN-β pre-treatment (w/IFN-β). (For interpretation of the references to color in this figure legend, the reader is referred to the Web version of this article.)

5. Conclusions

The application of an *Interferome*-based cell type-specific approach allowed us to identify IFN-linked pathways and cell mechanisms altered specifically in MS B cells and monocytes relevant to MS pathogenesis and maintenance that may have important implications on fate and functions of these cell types and that may also hold therapeutic potential for the development of novel strategies and combined protocols to treat MS targeting pathogenic function of specific cells.

In particular, having in mind the usage of IFN-β therapy in MS treatment and its ability to modulate monocyte-B cell crosstalk [32] or to specifically deplete the pathogenic $CD27^+$ memory B cell compartment [37], we might envisage the possibility of a synergistic effect of IFN-β therapy as add-on therapy with other drugs targeting B cells or the development and optimization of IFN-based immunocytokines [94] that may allow cell-specific modulation of altered IFN-linked processes in specific cell types impacting on immunopathogenic mechanisms and disease course.

Conflicts of interest

Severa M., Rizzo F., Srinivasan S., Di Dario M., Giacomini E., Buscarinu M.C., Cruciani M., Etna M.P., Sandini S., Mechelli R., Farina A., Trivedi P., Hertzog P.J. and Coccia E.M. declare no conflict of interest.

Farina C. received research support from Merck-Serono, Teva, Novartis.

Salvetti M. received research support and consulting fees from Biogen, Merck, Novartis, Roche, Sanofi, Teva.

Author contribution

M.S. isolated and cultured the cells for array analysis and validation experiments, performed the functional validation studies, analyzed and graphed the data, was involved in study design and experimental settings and wrote the manuscript. F.R. isolated and cultured the cells for array analysis and validation experiments and performed the functional validation studies. E.G. isolated the cells for array analysis. S.S. performed statistical and bioinformatics analyses. M.D.D. conducted microarray studies. M.C.B, R.M. and M.S. recruited the patients and matched healthy controls and obtained the relevant blood samples used in this study. M.C., M.P.E. and S.S. performed western blotting analyses. A.F. and P.T. cultured the GFP-tagged Epstein-barr virus strain and helped with infection settings. P.J.H. gave us full access to *Interferome* database. C.F. and E.M.C. were both involved in funding acquisition, study conceptualization and design as well as in the revision of the manuscript. E.M.C. supervised the whole study.

Data and materials availability

Raw microarray data will be provided upon request.

Acknowledgements

The authors acknowledge Dr. Silvia Romano, Dr. Arianna Fornasiero and Dr. Michela Ferraldeschi, of Saint Andrea Hospital MS Center (Sapienza University, Rome, Italy) who took care of patients and helped with sampling; the Flow Cytometry Facility (FAST, Istituto Superiore di Sanità, Rome, Italy) for technical support.

This work was supported by Fondazione Italiana Sclerosi Multipla (FISM grant 2013/R/9 to EMC and CF) and in part also by grant GR-2016-02363749 from Italian Ministry of Health (to MS).

Appendix A. Supplementary data

Supplementary data to this article can be found online at https://doi.org/10.1016/j.jaut.2019.04.006.

References

[1] R.M. Ransohoff, D.A. Hafler, C.F. Lucchinetti, Multiple sclerosis-a quiet revolution, Nat. Rev. Neurol. 11 (3) (2015) 134–142.
[2] R. Dobson, G. Giovannoni, Multiple sclerosis - a review, Eur. J. Neurol. 26 (1) (2019) 27–40.
[3] T. Olsson, L.F. Barcellos, L. Alfredsson, Interactions between genetic, lifestyle and environmental risk factors for multiple sclerosis, Nat. Rev. Neurol. 13 (1) (2017) 25–36.
[4] C. Munz, et al., Antiviral immune responses: triggers of or triggered by autoimmunity? Nat. Rev. Immunol. 9 (4) (2009) 246–258.
[5] A. Ascherio, K.L. Munger, Environmental risk factors for multiple sclerosis. Part I: the role of infection, Ann. Neurol. 61 (4) (2007) 288–299.
[6] S. Burnard, J. Lechner-Scott, R.J. Scott, EBV and MS: major cause, minor contribution or red-herring? Mult. Scler. Relat. Disord. 16 (2017) 24–30.
[7] G. Trinchieri, Type I interferon: friend or foe? J. Exp. Med. 207 (10) (2010) 2053–2063.
[8] L. Ronnblom, M.L. Eloranta, The interferon signature in autoimmune diseases, Curr. Opin. Rheumatol. 25 (2) (2013) 248–253.
[9] S. Kretschmer, M.A. Lee-Kirsch, Type I interferon-mediated autoinflammation and autoimmunity, Curr. Opin. Immunol. 49 (2017) 96–102.
[10] C. International Multiple Sclerosis Genetics, et al., Genetic risk and a primary role for cell-mediated immune mechanisms in multiple sclerosis, Nature 476 (7359) (2011) 214–219.
[11] P.L. De Jager, et al., Meta-analysis of genome scans and replication identify CD6, IRF8 and TNFRSF1A as new multiple sclerosis susceptibility loci, Nat. Genet. 41 (7) (2009) 776–782.
[12] International Multiple Sclerosis Genetics Consortium (IMSGC), Analysis of immune-related loci identifies 48 new susceptibility variants for multiple sclerosis, Nat.

Genet. 45 (2013) 1353–1360.
[13] S. Srinivasan, et al., Dysregulation of MS risk genes and pathways at distinct stages of disease, Neurol. Neuroimmunol. Neuroinflammation 4 (3) (2017) e337.
[14] S. Malhotra, et al., Search for specific biomarkers of IFNbeta bioactivity in patients with multiple sclerosis, PLoS One 6 (8) (2011) e23634.
[15] L.G. van Baarsen, et al., A subtype of multiple sclerosis defined by an activated immune defense program, Genes Immun. 7 (6) (2006) 522–531.
[16] K. Cervantes-Gracia, H. Husi, Integrative analysis of Multiple Sclerosis using a systems biology approach, Sci. Rep. 8 (1) (2018) 5633.
[17] S. Srinivasan, et al., Transcriptional dysregulation of interferome in experimental and human multiple sclerosis, Sci. Rep. 7 (1) (2017) 8981.
[18] K.D. Yamaguchi, et al., IFN-beta-regulated genes show abnormal expression in therapy-naive relapsing-remitting MS mononuclear cells: gene expression analysis employing all reported protein-protein interactions, J. Neuroimmunol. 195 (1–2) (2008) 116–120.
[19] D. Hesse, et al., Breakthrough disease during interferon-[beta] therapy in MS: No signs of impaired biologic response, Neurology 74 (18) (2010) 1455–1462.
[20] D. Hesse, et al., Disease protection and interleukin-10 induction by endogenous interferon-beta in multiple sclerosis? Eur. J. Neurol. 18 (2) (2011) 266–272.
[21] F. Sellebjerg, et al., Endogenous and recombinant type I interferons and disease activity in multiple sclerosis, PLoS One 7 (6) (2012) e35927.
[22] L.F. van der Voort, et al., Spontaneous MxA mRNA level predicts relapses in patients with recently diagnosed MS, Neurology 75 (14) (2010) 1228–1233.
[23] P. Mulero, L. Midaglia, X. Montalban, Ocrelizumab: a new milestone in multiple sclerosis therapy, Ther. Adv. Neurol. Disord. 11 (2018) 1756286418773025.
[24] K. Lehmann-Horn, S. Kinzel, M.S. Weber, Deciphering the role of B cells in multiple sclerosis-towards specific targeting of pathogenic function, Int. J. Mol. Sci. 18 (10) (2017).
[25] C.F. Lucchinetti, et al., Inflammatory cortical demyelination in early multiple sclerosis, N. Engl. J. Med. 365 (23) (2011) 2188–2197.
[26] L. Michel, et al., B cells in the multiple sclerosis central nervous system: trafficking and contribution to CNS-compartmentalized inflammation, Front. Immunol. 6 (2015) 636.
[27] H. Lassmann, Multiple sclerosis pathology, Cold Spring Harb. Perspect. Med. 8 (3) (2018).
[28] O. Stuve, et al., Long-term B-lymphocyte depletion with rituximab in patients with relapsing-remitting multiple sclerosis, Arch. Neurol. 66 (2) (2009) 259–261.
[29] S.L. Hauser, et al., B-cell depletion with rituximab in relapsing-remitting multiple sclerosis, N. Engl. J. Med. 358 (7) (2008) 676–688.
[30] L.M. Metz, et al., Trial of minocycline in a clinically isolated syndrome of multiple sclerosis, N. Engl. J. Med. 376 (22) (2017) 2122–2133.
[31] P.S. Sorensen, et al., Minocycline added to subcutaneous interferon beta-1a in multiple sclerosis: randomized Recycline study, Eur. J. Neurol. 23 (5) (2016) 861–870.
[32] E. Giacomini, et al., IFN-beta therapy modulates B-cell and monocyte crosstalk via TLR7 in multiple sclerosis patients, Eur. J. Immunol. 43 (7) (2013) 1963–1972.
[33] S.A. Samarajiwa, et al., Interferome: the database of interferon regulated genes, Nucleic Acids Res. 37 (Database issue) (2009) D852–D857.
[34] I. Rusinova, et al., Interferome v2.0: an updated database of annotated interferon-regulated genes, Nucleic Acids Res. 41 (Database issue) (2013) D1040–D1046.
[35] A.J. Thompson, et al., Diagnosis of multiple sclerosis: 2017 revisions of the McDonald criteria, Lancet Neurol. 17 (2) (2018) 162–173.
[36] E. Giacomini, et al., Thymosin-alpha1 expands deficient IL-10-producing regulatory B cell subsets in relapsing-remitting multiple sclerosis patients, Mult. Scler. (2017) 1352458517695892.
[37] F. Rizzo, et al., Interferon-beta therapy specifically reduces pathogenic memory B cells in multiple sclerosis patients by inducing a FAS-mediated apoptosis, Immunol. Cell Biol. 94 (9) (2016) 886–894.
[38] G. Dennis Jr.et al., DAVID: database for annotation, visualization, and integrated discovery, Genome Biol. 4 (5) (2003) P3.
[39] A. Kasprzyk, BioMart: Driving a Paradigm Change in Biological Data Management vol. 2011, Database, Oxford), 2011, p. bar049.
[40] M. Bessarabova, et al., Knowledge-based analysis of proteomics data, BMC Bioinf. 13 (Suppl 16) (2012) S13.
[41] P. Carmona-Saez, et al., Genecodis: a web-based tool for finding significant concurrent annotations in gene lists, Genome Biol. 8 (1) (2007) R3.
[42] M. Cruciani, et al., Staphylococcus aureus Esx factors control human dendritic cell functions conditioning Th1/Th17 response, Front. Cell. Infect. Microbiol. 7 (2017) 330.
[43] M.P. Etna, et al., Mycobacterium tuberculosis-induced miR-155 subverts autophagy by targeting ATG3 in human dendritic cells, PLoS Pathog. 14 (1) (2018) e1006790.
[44] A. Farina, et al., Epstein-Barr virus lytic infection promotes activation of Toll-like receptor 8 innate immune response in systemic sclerosis monocytes, Arthritis Res. Ther. 19 (1) (2017) 39.
[45] M. Severa, et al., Sensitization to TLR7 agonist in IFN-beta-preactivated dendritic cells, J. Immunol. 178 (10) (2007) 6208–6216.
[46] R.C. Taylor, S.P. Cullen, S.J. Martin, Apoptosis: controlled demolition at the cellular level, Nat. Rev. Mol. Cell Biol. 9 (3) (2008) 231–241.
[47] E.J. Hillmer, et al., STAT3 signaling in immunity, Cytokine Growth Factor Rev. 31 (2016) 1–15.
[48] D.S. Skundric, et al., Emerging role of IL-16 in cytokine-mediated regulation of multiple sclerosis, Cytokine 75 (2) (2015) 234–248.
[49] C.E. Samuel, Antiviral actions of interferons, Clin. Microbiol. Rev. 14 (4) (2001) 778–809 (table of contents).
[50] Y. Nakaya, et al., AIM2-like receptors positively and negatively regulate the interferon response induced by cytosolic DNA, mBio 8 (4) (2017).
[51] T. Regad, M.K. Chelbi-Alix, Role and fate of PML nuclear bodies in response to interferon and viral infections, Oncogene 20 (49) (2001) 7274–7286.
[52] S. Akira, K. Hoshino, Myeloid differentiation factor 88-dependent and -independent pathways in toll-like receptor signaling, J. Infect. Dis. 187 (Suppl 2) (2003) S356–S363.
[53] J.W. Darnowski, et al., Stat3 cleavage by caspases: impact on full-length Stat3 expression, fragment formation, and transcriptional activity, J. Biol. Chem. 281 (26) (2006) 17707–17717.
[54] A. Elssner, et al., IL-16 is constitutively present in peripheral blood monocytes and spontaneously released during apoptosis, J. Immunol. 172 (12) (2004) 7721–7725.
[55] L.S. Young, A.B. Rickinson, Epstein-Barr virus: 40 years on, Nat. Rev. Canc. 4 (10) (2004) 757–768.
[56] M.K. Crow, Type I interferon in organ-targeted autoimmune and inflammatory diseases, Arthritis Res. Ther. 12 (Suppl 1) (2010) S5.
[57] K.A. Kirou, et al., Activation of the interferon-alpha pathway identifies a subgroup of systemic lupus erythematosus patients with distinct serologic features and active disease, Arthritis Rheum. 52 (5) (2005) 1491–1503.
[58] D.J. Gough, et al., Constitutive type I interferon modulates homeostatic balance through tonic signaling, Immunity 36 (2) (2012) 166–174.
[59] X. Feng, et al., Type I interferon signature is high in lupus and neuromyelitis optica but low in multiple sclerosis, J. Neurol. Sci. 313 (1–2) (2012) 48–53.
[60] X. Feng, et al., Low expression of interferon-stimulated genes in active multiple sclerosis is linked to subnormal phosphorylation of STAT1, J. Neuroimmunol. 129 (1–2) (2002) 205–215.
[61] J. Ahn, et al., Abnormal levels of interferon-gamma receptors in active multiple sclerosis are normalized by IFN-beta therapy: implications for control of apoptosis, Front. Biosci. 9 (2004) 1547–1555.
[62] T. Bose, Role of immunological memory cells as a therapeutic target in multiple sclerosis, Brain Sci. 7 (11) (2017).
[63] M.T. Boylan, et al., CD80 (B7-1) and CD86 (B7-2) expression in multiple sclerosis patients: clinical subtype specific variation in peripheral monocytes and B cells and lack of modulation by high dose methylprednisolone, J. Neurol. Sci. 167 (2) (1999) 79–89.
[64] R. Gonzalez-Amaro, et al., Is CD69 an effective brake to control inflammatory diseases? Trends Mol. Med. 19 (10) (2013) 625–632.
[65] O. McWilliam, et al., B cells from patients with multiple sclerosis have a pathogenic phenotype and increased LTalpha and TGFbeta1 response, J. Neuroimmunol. 324 (2018) 157–164.
[66] J. Satoh, et al., Microarray analysis identifies a set of CXCR3 and CCR2 ligand chemokines as early IFNbeta-responsive genes in peripheral blood lymphocytes in vitro: an implication for IFNbeta-related adverse effects in multiple sclerosis, BMC Neurol. 6 (2006) 18.
[67] I. Smets, et al., Multiple sclerosis risk variants alter expression of co-stimulatory genes in B cells, Brain 141 (3) (2018 Mar 1) 786–796.
[68] T.L. Sorensen, F. Sellebjerg, Distinct chemokine receptor and cytokine expression profile in secondary progressive MS, Neurology 57 (8) (2001) 1371–1376.
[69] M.S. Weber, et al., Multiple sclerosis: glatiramer acetate inhibits monocyte reactivity in vitro and in vivo, Brain 127 (Pt 6) (2004) 1370–1378.
[70] B. Macchi, et al., Role of inflammation and apoptosis in multiple sclerosis: comparative analysis between the periphery and the central nervous system, J. Neuroimmunol. 287 (2015) 80–87.
[71] S.J. Riedl, Y. Shi, Molecular mechanisms of caspase regulation during apoptosis, Nat. Rev. Mol. Cell Biol. 5 (11) (2004) 897–907.
[72] B. Macchi, et al., Impaired apoptosis in mitogen-stimulated lymphocytes of patients with multiple sclerosis, Neuroreport 10 (2) (1999) 399–402.
[73] M. Moreno, et al., Activation-induced cell death in T lymphocytes from multiple sclerosis patients, J. Neuroimmunol. 272 (1–2) (2014) 51–55.
[74] E. Julia, et al., Differential susceptibility to apoptosis of CD4+T cells expressing CCR5 and CXCR3 in patients with MS, Clin. Immunol. 133 (3) (2009) 364–374.
[75] A. Mathias, et al., Increased ex vivo antigen presentation profile of B cells in multiple sclerosis, Mult. Scler. 23 (6) (2017) 802–809.
[76] A.T. Reder, et al., Monocyte activation in multiple sclerosis, Mult. Scler. 4 (3) (1998) 162–168.
[77] Z.A. Nagy, N.A. Mooney, A novel, alternative pathway of apoptosis triggered through class II major histocompatibility complex molecules, J. Mol. Med. (Berl.) 81 (12) (2003) 757–765.
[78] M.S. Weber, et al., Type II monocytes modulate T cell-mediated central nervous system autoimmune disease, Nat. Med. 13 (8) (2007) 935–943.
[79] W. Cruikshank, F. Little, lnterleukin-16: the ins and outs of regulating T-cell activation, Crit. Rev. Immunol. 28 (6) (2008) 467–483.
[80] S. Rahangdale, et al., Chemokine receptor CXCR3 desensitization by IL-16/CD4 signaling is dependent on CCR5 and intact membrane cholesterol, J. Immunol. 176 (4) (2006) 2337–2345.
[81] G.L. Chupp, et al., Tissue and T cell distribution of precursor and mature IL-16, J. Immunol. 161 (6) (1998) 3114–3119.
[82] S. Nischwitz, et al., Interferon beta-1a reduces increased interleukin-16 levels in multiple sclerosis patients, Acta Neurol. Scand. 130 (1) (2014) 46–52.
[83] D.S. Skundric, et al., Production of IL-16 correlates with CD4+ Th1 inflammation and phosphorylation of axonal cytoskeleton in multiple sclerosis lesions, J. Neuroinflammation 3 (2006) 13.
[84] Y. Zhang, et al., Processing and activation of pro-interleukin-16 by caspase-3, J. Biol. Chem. 273 (2) (1998) 1144–1149.
[85] D.S. Skundric, W.W. Cruikshank, J. Drulovic, Role of IL-16 in CD4+ T cell-mediated regulation of relapsing multiple sclerosis, J. Neuroinflammation 12 (2015) 78.
[86] D.S. Skundric, et al., Distinct immune regulation of the response to H-2b restricted epitope of MOG causes relapsing-remitting EAE in H-2b/s mice, J. Neuroimmunol.

136 (1–2) (2003) 34–45.
[87] A.L. Greenfield, S.L. Hauser, B-cell therapy for multiple sclerosis: entering an era, Ann. Neurol. 83 (1) (2018) 13–26.
[88] M. Laurence, J. Benito-Leon, Epstein-Barr virus and multiple sclerosis: updating Pender's hypothesis, Mult. Scler. Relat. Disord. 16 (2017) 8–14.
[89] H.H. Niller, H. Wolf, J. Minarovits, Regulation and dysregulation of Epstein-Barr virus latency: implications for the development of autoimmune diseases, Autoimmunity 41 (4) (2008) 298–328.
[90] B. Serafini, et al., Epstein-Barr virus latent infection and BAFF expression in B cells in the multiple sclerosis brain: implications for viral persistence and intrathecal B-cell activation, J. Neuropathol. Exp. Neurol. 69 (7) (2010) 677–693.
[91] A. Hassani, et al., Epstein-Barr virus is present in the brain of most cases of multiple sclerosis and may engage more than just B cells, PLoS One 13 (2) (2018) e0192109.
[92] R. Mechelli, et al., A "candidate-interactome" aggregate analysis of genome-wide association data in multiple sclerosis, PLoS One 8 (5) (2013) e63300.
[93] Y. Tao, X. Zhang, S. Markovic-Plese, Toll-like receptor (TLR)7 and TLR9 agonists enhance interferon (IFN) beta-1a's immunoregulatory effects on B cells in patients with relapsing-remitting multiple sclerosis (RRMS), J. Neuroimmunol. 298 (2016) 181–188.
[94] A. Cauwels, et al., Targeting interferon activity to dendritic cells enables in vivo tolerization and protection against EAE in mice, J. Autoimmun. 97 (2019) 70–76.